Resilient Cities and Structures 1 (2022) 76–86

Contents lists available at ScienceDirect

Resilient Cities and Structures

journal homepage: www.elsevier.com/locate/rcns

Resilience of city underground infrastructure under multi-hazards impact: From structural level to network level

Hongwei Huang, Dongming Zhang*, Zhongkai Huang

Key Laboratory of Geotechnical and Underground Engineering of Minister of Education, Department of Geotechnical Engineering and International Joint Research Center for Resilient Infrastructure, Tongji University, Shanghai, 200092, China

ARTICLE INFO

Keywords:
Underground infrastructure
Resilience
Multi-hazards
Structure
Network

ABSTRACT

Underground infrastructure (UI) plays a great important role in the urbanization and modernization of megacities in the world. However, the intensive development of the UI during the past decades has posed great risks to the safety of city infrastructures under the impact of multi-hazards, especially with the condition of global climate change. In this paper, a general conceptualized framework to assess the resilience of UI in cities under multi-hazards impact is proposed. The urban tunnel system, e.g., metro tunnel, road tunnel etc., is selected as the typical underground infrastructure discussed with the emphasis both on the structural level in terms of mechanical behaviors and system level in terms of network efficiency. The hazards discussed in this paper include the natural hazards and human-related ones, with emphasis on earthquake, flood, and aggressive disturbances caused by human activities. After the general framework proposed for resilience of the structural and network behavior of the UI, two application examples are illustrated. The structural resilience of the shield tunnel under earthquake impact is analyzed by using the proposed resilience model, and the network resilience of the road tunnel system under the flood impact due to climate change is analyzed, respectively. The resilience enhancement by using the adaptive design strategy of real-time observational method is mathematically presented in this case. Some other practical engineering recovery measures are briefly discussed at the end of this application example. The findings in the application examples should be helpful to enhance the resilience-based design of the structural and network of tunnels from the component to the system level.

1. Introduction

In recent decades, the investment in underground infrastructure (such as metro systems, underwater long tunnels, and urban underground pipelines) has been increasing all overtime in the world. This development is extremely fast in China, with a total area of constructed underground space at about 2.4 billion m^2 and an increment of only one year at 2020 is about 0.3 billion m^2 from the statistics of underground space report [1]. As the physical carrier of national economic development for a long time, the underground infrastructure development has gradually changed from a single node project as one tunnel to networked systems spanning the whole community such as metro tunnel in the city or even cross over cities. It has no doubt to conclude the underground infrastructure is a huge system nowadays to provide the basic function of a big city, including the transportation, power supply, water supply, and so on.

However, Moser [2], who is the world bank officer, has pointed out that the asset vulnerability would be negatively correlated with its increasing development of the asset scales. The more complex of the assets (such as underground infrastructure) is, the more vulnerable the system would be. The underground infrastructure that has been built and put into operation on a large scale is intensively affected by the multiple hazards, such as global climate change, earthquakes, floods, and other natural disasters [3–6]. For example, the 2008 Wenchuan earthquake in China has destroyed quite a number of tunnels to different degrees of the vulnerability, which stopped the emergency lifeline supply from the safety places [7]. In 2021, the extremely heavy rainfall in a relatively short time in Zhengzhou city of China has raised the water level and flood the entrance of the tunnel portal of metro lines, which caused a severe tragedy of 12 death and five injuries in the metro trains which is covered by flooded waters in the tunnel [8]. However, despite of those natural hazards, the most frequently encountered threats to the operated underground infrastructures are coming from the nearby disturbance induced by the human activities. A typical example is the deep excavation for high-rise buildings near the metro lines nowadays in cities [9]. The Shanghai metro tunnels have experienced more than 2000 cases of the nearby excavation or surcharges that are unexpected additional loadings on the running underground infrastructures [10]. Those “black swan” impacts [11] would not only influence on the well-design structures but also affect the entire network efficiency. The above threats either com-

* Corresponding author.
E-mail addresses: huanghw@tongji.edu.cn (H. Huang), 09zhang@tongji.edu.cn (D. Zhang), 5huangzhongkai@tongji.edu.cn (Z. Huang).

https://doi.org/10.1016/j.rcns.2022.07.003
Received 1 June 2022; Received in revised form 16 July 2022; Accepted 16 July 2022
Available online 25 July 2022

ing from the natural hazards or from the human-related activities would require the engineers to reveal the safety design of the underground infrastructures during their entire life span. The safety is required not only in the stage of pre-disaster, but also during the disaster and even after the disaster. Different from the connotation of traditional risk management and control, the research on the resilience of infrastructure focuses on the ability of infrastructure to resist risk challenges, which is a promotion change from the traditional passive risk control to the active resilience. In view of this circumstance, the recent extensive researches on the resilience of the communities and civil structures could be a promising direction to cover both the risk analysis before the hazards and the rapid recovery after the hazards [12–13]. Resilience is a kind of capability and characteristic of the system, which can be used to describe the ability of the system to keep balance after being disturbed by the outside or to quickly and efficiently return to the equilibrium after the balance is broken [14]. ASCE [15] believes that resilience is one of the 8 basic standards for civil engineering facilities. National Academy of Sciences of the United States [16] defines resilience as the ability to prevent, bear, recover and adapt to adverse events. The construction of resilient underground infrastructure is the next important development direction for traditional civil engineering under the background of new situation and new technology.

Although the needs for a resilient underground infrastructure is quite urgent, however, the detailed researches on the topic is limited so far. The gap between the needs and the researches lies on the clear definition of the resilience metric associated with the system indicators to describe the performance of the underground infrastructures. Quite a number of literatures has proposed a resilience evaluation model of civil infrastructure with the resilience index defined by the area ratio of the loss of performance area over the area covered by the initial performance curve [17–20]. Huang et al. [14] has updated the above resilience evaluation model by considering the evolution stage between the disruption stage and the recovery stage for the time of decision making and specifically applied this new model to a shield tunnel structure in Shanghai. Sangaki et al. [21] presented a probabilistic framework and models that can consider the effect of uncertainties in the seismic resilience index. Mottahedi et al. [22] developed a practical methodology to estimate resilience based on the combination of expert judgment and fuzzy set theory. However, it should be admitted that the above analysis or proposed resilience model is mostly for the infrastructure above the ground and specifically for a single node of the structures, such as a structural frame or a tunnel ring, which might not be sufficient to represent the engineering needs to assess the resilience ability of the underground infrastructure under the multi-hazards conditions.

To narrow the gap between the above needs and the current literature limitations, this paper tries to propose an overall framework to evaluate the resilience of the underground infrastructure where the tunnel system is highlighted. Firstly, the definition of the resilience for the underground infrastructure system is proposed and discussed with different levels of the tunnel system from the structure component to the network system. Then the system performance indicators under multi-hazards are discussed with emphasis on the earthquake, flood and human-related aggressive activities. Then the structural seismic resilience and the network resilience is specifically analyzed by two illustrative examples for the applicability of the general framework. The enhancement solutions to improve the resilience is discussed in the application example in the end of this paper.

2. Definition and metrics of underground infrastructure resilience

The resilience is explained conceptually as the ability of a system to absorb the disruption caused by hazards and the ability to recover to an acceptable performance level [23–25] . In line with this widely accepted definition, the resilience of UI could exhibit the ability of the infrastructure system to absorb the disruption caused by multi hazards and the corresponding ability to recover to an engineering practical level

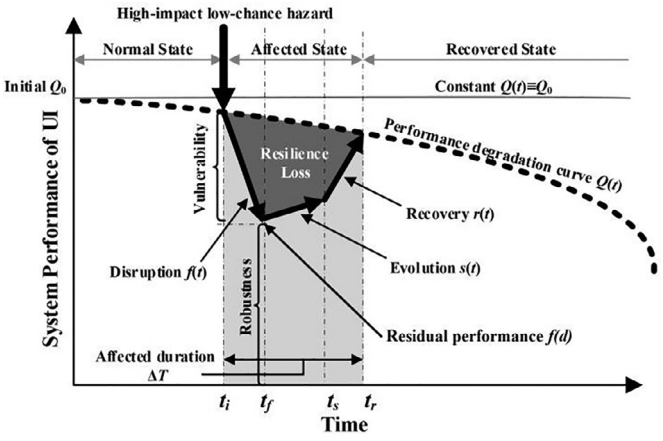

Fig. 1. General definition and metric to quantify the resilience of UI.

of the system performance of the UI. The resilience of UI under multiple hazards could be further categorized into two major types in terms of the different definitions of the system performance. The system performance could be varied with respect to the infrastructure scale, e.g., structural component level or system network level, as well as to the specific hazard type, e.g., performance under seismic, fire, flood, or engineering disturbances, which will be discussed in details in the next section. However, the metrics of resilience model given different types of system performance should be unified and generally explained in Fig. 1.

Fig. 1 has illustrated the detailed frame of lifetime performance evolution for underground infrastructure. The overall lifetime performance could be divided into three conditions before the hazard, during the hazard and after the hazard. The metric of the resilience model is mainly focused on the time interval during the hazard shown as the shaded area in Fig. 1. Given an action coming from a high-impact but low-chance hazard on the UI, in general, there are three stages to quantify the resilience metric including disruption stage, evolution stage and recovery stage. Once the hazard is occurred at time t_i, the infrastructure will make a response to this action. The performance will decrease shown by function $f(t)$. The residual performance f_d after this response (at time t_f) stands for the robustness of the system. Due to the time needs for the decision-making including investigation, discussion and decision on the recovery measures, the performance will be exhibited in a stage described by function $s(t)$. Then, once the recovery is conducted at time t_s, the recovery will take place until the time t_r to an acceptable level of performance. Hence, the metric of resilience of UI can be visually explained by the ratio of the area for the performance function group including $f(t)$, $s(t)$ and $r(t)$, over the area of normal performance function $Q_n(t)$. The resilience index can be thus calculated by following equation:

$$\mathrm{Re} = \frac{t_f - t_i}{t_r - t_i} F + \frac{t_s - t_f}{t_r - t_i} S + \frac{t_r - t_s}{t_r - t_i} R \tag{1a}$$

$$F = \frac{\int_{t_i}^{t_f} f\,dt}{\int_{t_i}^{t_f} Q\,dt} \tag{1b}$$

$$S = \frac{\int_{t_f}^{t_s} s\,dt}{\int_{t_f}^{t_s} Q\,dt} \tag{1c}$$

$$R = \frac{\int_{t_s}^{t_r} r\,dt}{\int_{t_s}^{t_r} Q\,dt} \tag{1d}$$

The typical dimensions under resilience concept can be covered in the above metric of the resilience, including degradation, robustness, vulnerability, rapidity and recovery. Details are summarized in Table 1.

Table 1
Resilience dimension and its property.

Dimension	Symbol	Property
Degradation	f_i	Degraded performance $Q_n(t)$ at t_i
Robustness	f_d	Residual performance at t_f
Vulnerability	f_i=f_i-f_d	Performance loss at t_f
Rapidity	ΔT=t_r-t_s	Speed of recovery
Recovery	f_r	Recovered performance

3. Performance indictors of underground infrastructure

It should be noted that different types of underground infrastructure have different performance indicator Q under different types of the multi-hazards. Different performance indictor Q will then determine the corresponding index of resilience metric Re. In general, Table 2 has illustrated some typical examples of the performance indicator for different types of infrastructure functions. For the underground infrastructures, the earthquake and flood are the two frequently encountered natural hazards, while the engineering disturbances are the frequently encountered man-made hazards. Hence, in the following of this section, the details of the structural performance under seismic hazard, man-made hazard in terms of the engineering disturbance near the underground infrastructures will be discussed in the component level while the network performance indicator under the flood hazard will be discussed in the system level.

3.1. Structural performance of UI

3.1.1. Fragility curve based seismic performance

The seismic resilience of underground infrastructure is mainly referred to the structure component exposed to a given seismic intensity level (intensity measure, e.g., *IM*) that can bear the vulnerability by using the fragility functions and recover to its certain restoration functions. The seismic performance is thus represented by the fragility function and restoration functions respectively. It is slightly different from Fig. 1 that the performance at the disruption stage is always assumed to be instantaneous at the moment when the earthquake occurs. The seismic performance $Q(t)$ for earthquake impact on the underground infrastructure can be represented by the followings:

$$Q(t) = \sum_{j=1}^{4} Q\left[DS_j|t\right] P\left[DS_j|IM\right] \tag{2}$$

where $Q\ [DS_j|t]$ means the function of UI to restore the functionality at time t and damage stage j, and $P\ [DS_j|IM]$ is referred to the conditional probability of the specific damage state j for an event given with the intensity measure (*IM*). Four types of damage stages were identified by the variation of the ratio of acting bending moment (M_{sd}) over the capacity bending moment (M_{Rd}), namely minor(d_{S1}), moderate (d_{S2}), extensive (d_{S3}) and complete (d_{S4}) [22] damage. Details of the calculation for the Q and P under different level of *IM* can be specifically referred to the literature [26–27], which is not elaborated here. It should be specifically noted that the functionality Q here is a general concept which can be any type of interested function of the underground infrastructure when it is subjected to the earthquake. But the conditional probability P is based on the seismic vulnerability analysis which considers the fragility curves under different levels of the seismic intensity (*IM*). Hence, the seismic performance indicator discussed in this paper is referred to the fragility curve based on seismic performance.

$$Q(t) = \frac{\Delta D_0}{\Delta D(t)}$$

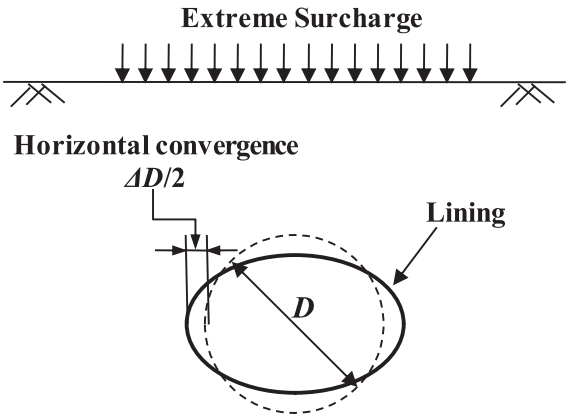

Fig. 2. Performance indicator of structural deformation of UI.

3.1.2. Deformational performance under human-related disturbance

The structure deformation is normally used as an indicator for the assessment of the service performance of underground infrastructure. For the illustrative perspective in this paper, the structural deformation of metro tunnel, e.g., one typical underground infrastructure, is discussed in details. Based on a statistic from Shanghai metro [14], the unexpected surcharge on the ground surface above the tunnel and the nearby deep excavation around the tunnel should be the two most significant man-made hazards that will impact on the structural performance of the operational tunnel. The disturbance coming either from the surcharge or from the excavation could be regarded as the additional loading and unloading effect on the tunnel lining. Thus, the tunnel horizontal convergence ΔD could be seen as a suitable indictor for the structural performance. Fig. 2 has shown the definition of horizontal convergence. Accordingly, the performance index $Q(t)$ by a normalization transformation form with ΔD, where ΔD_0 is the initial convergence deflection once the tunnel is built and $\Delta D(t)$ is the convergence at time t which can consider the degradation effect with time.

$$Q(t) = \frac{\Delta D_0}{\Delta D(t)} \tag{3}$$

Apart from the structural deformation, the capacity in terms of the mobilized strength is also concerned seriously. Hence, to consider the overall effect combining the deformational behavior and the stress-strain behavior, the structural energy can be regarded as the performance indicator as well.

$$Q(t) = 1 - \frac{\Pi_t}{\Pi_s} = 1 - \frac{\int_V \sigma_{ij}(t)\delta\varepsilon_{ij}(t)dV}{\int_V \tau_s \delta\varepsilon_s dV} \tag{4}$$

where Π_t/Π_s is referred to the mobilized ratio of the energy given the engineering disturbance from the surrounding environment. In this mo-

Table 2
Performance indictor for different type of underground infrastructure [23] .

System	Performance	Units
Structures	Space availability	Area per day
Transportation infrastructure	Traffic volume	Cars/passengers per day
Water treatment system	Water available for consumption	Volume per day
Utility network	Power delivered	Power per day

bilized ratio, the Π_t is the potential energy of the infrastructure considering the current status of stress and strain level, while the Π_s is the capacity limit of the potential energy that the infrastructure would go to the failure status. The performance indicator $Q(t)$ in Eq. (4) is basically referred to the change of potential energy of the system Π. The potential energy Π can be calculated by the integral of a mass body with each element represented by the multiplication of the stress σ_{ij} with the virtual strain $\delta\varepsilon_{ij}$ at time t. When the stress is replaced by the strength of the structural material, i.e., t_s, accordingly, the strain then will be at $\delta\varepsilon_s$, then the potential energy should be regarded as the capacity Π_s. When the structural potential energy mobilized is close to its capacity, the ratio will be close to unit. In that case, the energy performance Q would be reduced greatly to reflect the disruption both in the sense of strength and deformation.

3.2. Network performance of UI

3.2.1. Efficiency of network connectivity

With the large-scale networked development of underground infrastructure, the consequence of structural failure is not limited to a single node, but often has a great impact on the entire system. The tool of topology theory, as the basis for studying the network characteristics and functions, could maps various real network graphs in real life into simplified topology diagrams. It is usually composed of nodes and lines, where nodes represent individual structures in the system and lines represent the long linear structures connecting the individual structure. Based on topological networks, complex network theory can describe various internal interactions or relations of complex systems and analyze the performance of networks. The intensive underground infrastructures, such as the metro system and road tunnel system, can be regarded as a complex network composed of a large number of nodes and links. The node in metros could be the stations, while nodes in road tunnel system could be the tunnels. The links in metros could be the tunnels, while the links in the road tunnel system could be the roads.

The method of space L [28] in the topological modeling is adopted to construct the network of underground infrastructure in this paper due to its clear definition of the node and link in space L network corresponding to its physical meaning of the metro and road network. In complex network theory, adjacency matrix is used to express the connectivity between nodes in finite networks. Since the network is undirected, the adjacency matrix is symmetric and the diagonal elements are zero. In the underground infrastructure network, the weight assigned to the line is the actual length of the corresponding links between two adjacent nodes. Elements in the line-weighted adjacency matrix are equal to the weights on the line, as follows:

$$A_{ij} = \begin{cases} 0 & \text{if } i = j, \\ l_{ij}, & \text{the actual length of the line connecting nodes i and j,} \\ \infty & \text{otherwise.} \end{cases} \quad (5)$$

Network efficiency is used to measure network performance. Latora and Marchiori [29] defined global network efficiency as:

$$E_f = \frac{1}{N(N-1)} \sum_{i \neq j} \frac{1}{d_{ij}} \quad (6)$$

Where, N represents the total number of nodes; d_{ij} is the shortest path length between nodes i and j. The path length could be derived from the adjacency matrix from Eq. (5). The shortest path is the minimum of the summary of the actual length from node i to node j. The global network efficiency of Eq. (6) is equal to the mean of the shortest path between any two nodes in the whole network. On the basis of Eq. (6), the weighted network efficiency could further be proposed by considering the passenger flow volume effect on each node or link as following [30]:

$$E_f = \frac{1}{N(N-1)} \sum_{i \neq j} \frac{\omega_{ij}}{d_{ij}} \quad (7)$$

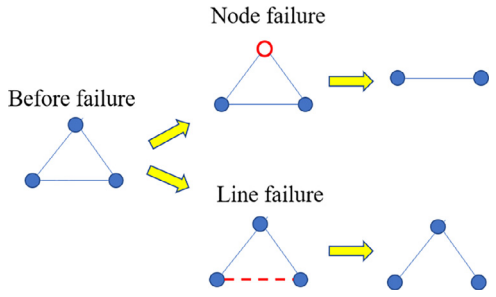

Fig. 3. Metro network failure mode.

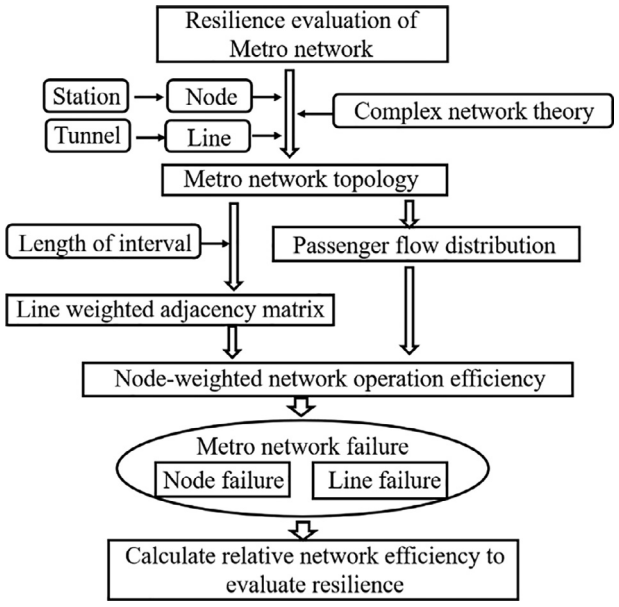

Fig. 4. Evaluation framework of metro network resilience.

where ω_{ij} is the node weight, which represents the passenger flux between node i and j. The influence of failure events on network performance is evaluated by relative network efficiency. Hence, network performance Q of UI could be defined as the ratio of post-fault network efficiency (E_f') to initial network efficiency (E_f^0):

$$Q(t) = \frac{E'_f(t)}{E_f^0} \quad (8)$$

3.2.2. Failures of metro network

Based on the characteristics of station distribution and tunnel connectivity of metro system, complex network theory can be used to analyze its performance. In metro topology network, nodes represent stations and lines represent interval tunnels. The length of the line (d_{ij} in Eq. (7)) is proportional to the actual distance between the corresponding two adjacent stations, and the node size is proportional to the number of passengers entering the station. Metro network failures can be simulated by removing some corresponding nodes and lines from the network, as shown in Fig. 3, thus leading to the decrease of network efficiency from two aspects. On the one hand, some stations lose connection and passenger flow. According to Eqs. (5) and (7), the path length of disconnected node pairs d_{ij} becomes infinite and ω_{ij} becomes zero. On the other hand, the shortest path between some stations becomes longer, that is, the d_{ij} of several node pairs increases. The characterization of the performance variation of the network under the failures could be presented in the following flowchart in Fig. 4.

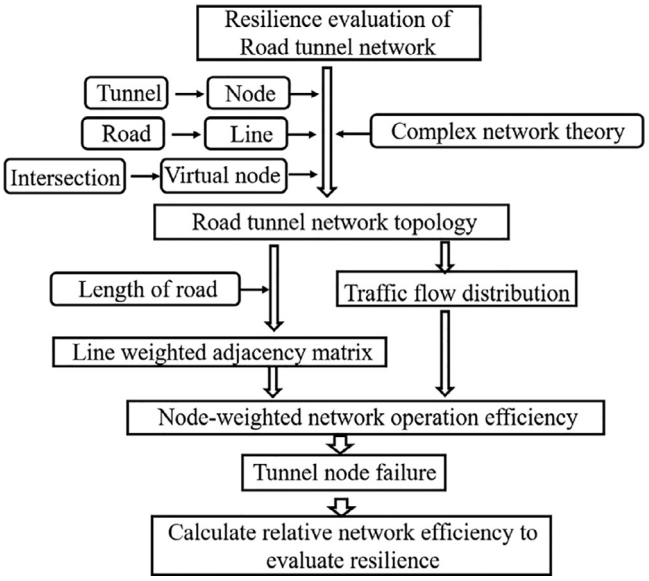

Fig. 5. Evaluation framework of road tunnel network resilience.

3.2.3. *Failures of road tunnel network*

Different from metro tunnels, road tunnels are mainly distributed sparsely in the road tunnel network. Therefore, when establishing the road traffic topology network, tunnels can be mapped as nodes according to the addresses. In addition, if the tunnel on a specific main road is destroyed, the nodes on the road can still be reached through other road sections and intersections, that is to say, if the tunnel node fails but the nodes on the same road do not fail at the same time, then the intersection can be regarded as "*virtual node*". It is assumed that this type of node will not suffer any damage cascading from the failures of nearby road tunnel and is only used to connect the road traffic network. The links in the network are representing the road sections between all nodes. The entire road tunnel network includes the node representing the real road tunnel, virtual node representing the road sections near the intersections and the link representing the road. After constructing the road tunnel topology network, similar to the metro tunnel network, considering road length and traffic flow distribution, adjacency matrix is obtained by the weight of road length to line, and the network efficiency is obtained the by weight of traffic flow to evaluate network resilience by Eq. (7).

When considering the failure of tunnel nodes in road tunnel network, the failure form can be regarded as that the damaged tunnel node loses all its related line connections and the traffic flow on its nodes, that is, the correlation d_{ij} becomes infinite and ω_{ij} becomes zero, similar with the concept of Fig. 3. At the same time, the destruction of tunnel nodes will also cause the shortest path between other network nodes to become longer, both of which will lead to the decrease of the operation efficiency of road tunnel network. The calculation flowchart of resilience and the performance of the road tunnel network is shown as following in Fig. 5.

4. Application example of metro tunnel lining subject to seismic hazard

In this section, the seismic resilience of the tunnel linings of metro is evaluated based on the model discussed in the previous sections including the resilience index (Eq. 1) and the seismic performance indicator (Eq. (2)). The framework of resilience analysis model combines the fragility and restoration functions, for assessing the robustness of tunnels exposed to different seismic scenarios, and the rapidity of the recovery considering different damage levels [31]. Fig. 6 is the flowchart of the general evaluation procedure, including the four steps: (i) hazard analysis and definition of the hazard intensity, based on available hazard curves or other relevant studies for the examined tunnel sites; (ii) the seismic vulnerability assessment, by adopting proper fragility functions (e.g., fragility curves), which assess the robustness of the structure and hence the loss of its functionality for given hazard intensities; (iii) the

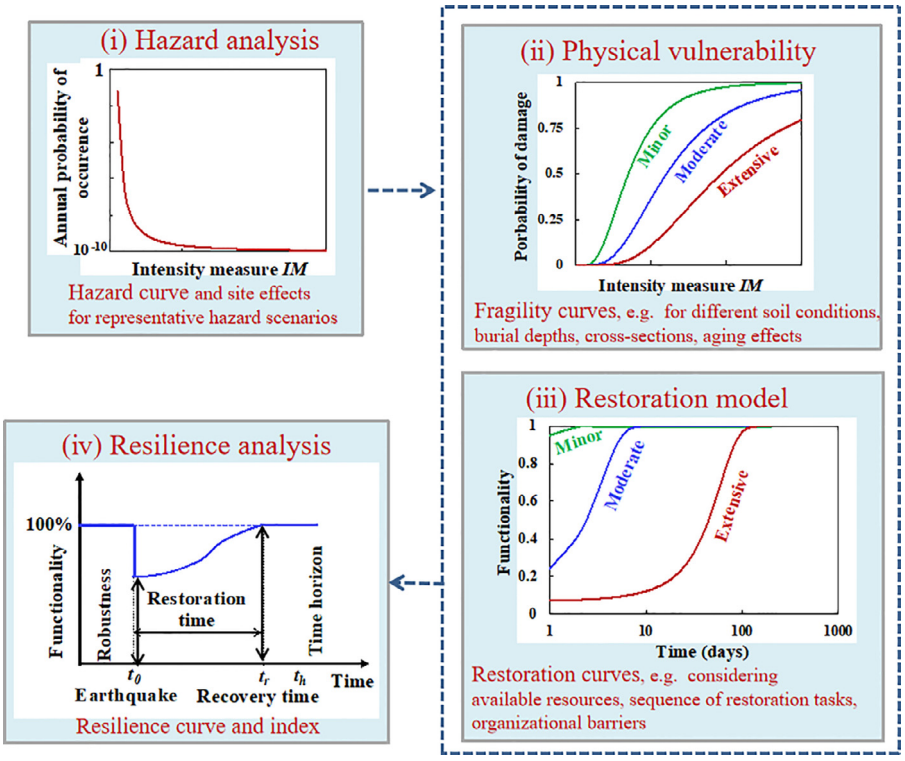

Fig. 6. Seismic resilience assessment framework of metro tunnels [31].

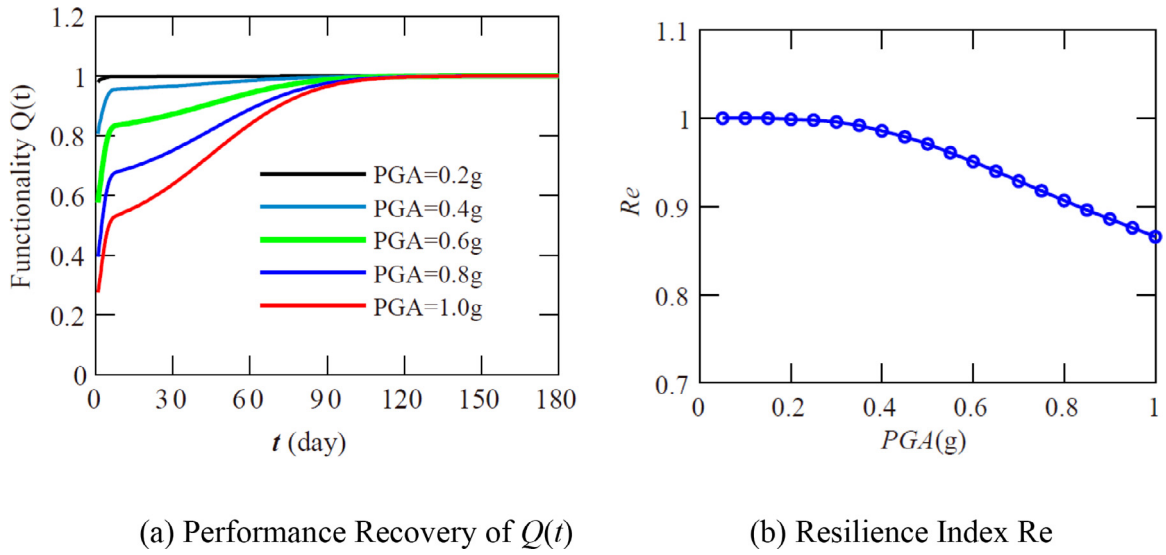

Fig. 7. Resilience analysis for Shanghai metro tunnel under different levels of *PGA*.

estimation of restoration time, which describes the rapidity of recovery after the occurrence of a hazard event, by including adequate restoration models and (iv) the resilience analysis and quantification with resilience metrics.

The above assessment procedure is applied into a typical Shanghai metro tunnel, where the tunnel is buried 9 m below the ground surface with a diameter of 6.2 m and a lining thickness of 0.35 m. The ground is typical Shanghai soft clay with an average of shear wave velocities at 200 m/s, an average density at 1.8 t/m^3, an average cohesion at 20 kPa and an average friction angle at 20 ° The fragility curves are derived via ABAQUS at different level of seismic intensity (IM). The details of the above simulation are illustrated by Huang [27] , which is not elaborated here. According to Eq. (2), the tunnel functionality $Q(t)$ at time t is calculated by the developed fragility curves and functionality restoration functions [32] considering the four types of the damage states. Fig. 7a shows the calculated tunnel performance $Q(t)$ subjected to different levels of seismic intensity which is represented by the five values of Peak Ground Acceleration (*PGA*) from 0.2 to 1.0 g. It is found that the damage induced by a lower seismic intensity seems to be more easily recovered from. Accordingly, Fig. 7b shows the resilience index *Re* evolution for the examined tunnel at different *PGA* levels. It is quite obvious that the seismic resilience index of the metro tunnel decreases gradually when the *PGA* increases. Given the condition of real design level of *PGA* in Shanghai practice around 0.1 g, it can be inferred from the figure that the resilience status of the Shanghai metro tunnel is relatively good.

5. Application example of road tunnel network subjected to flood hazard

5.1. Vulnerability analysis of typical road tunnel network in Suzhou city

Floods are one of the deadliest type of disasters in the world, accounting for 43.5% of disaster deaths despite large-scale flood control efforts [33]. The frequency of destructive floods in China is extremely high as well, and the economic loss has been increasing in recent decades [34]. Since the 1990s, the annual proportion of destructive floods in GDP has been 1.42%, nearly 40 times that of the United States [35]. Therefore, the resilience of underground infrastructure under flood is of great significance to ensure the safety of people's lives and property, in particular with the fact that the underground infrastructure is mostly below the ground surface level which is prone to converge the ground water into the entrance or exit of underground infrastructure during the heavy storms or water level rise.

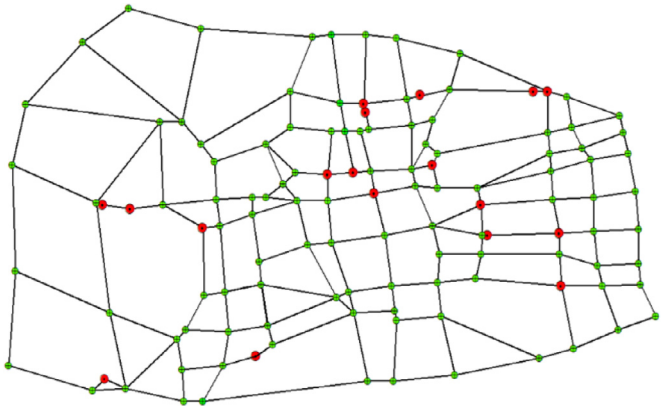

Fig. 8. Topographical map of road tunnel network in Suzhou.

Road tunnel is a major type of underground infrastructure. It is widely accepted that flood is a common natural disaster which has great influence on safe operation of road tunnels. For flat terrain and developed water distribution areas, road tunnel network is facing higher risk of flood disaster. Therefore, in this paper, the operational efficiency and resilience of a typical road tunnel network based on the inundation of road tunnel caused by extreme heavy rainfall is analyzed for the city of Suzhou in China. By using the topological mapping techniques, the location at the road tunnel and intersection are regarded as nodes, and the road sections between nodes are simulated by lines. Based on the actual geographical location information, the topology map of Suzhou urban transportation network including tunnels is constructed, as shown in Fig. 8. The green node is the intersection of each road section and is regarded as a "virtual node" in the topology, the red nodes shown in Fig. 8 are the road tunnel nodes, and the black link are line whose length is proportional to the actual distance between nodes.

As the water will find its way to come to the tunnel in its shortest path, hence, the flood is represented by the general water level rise on the basis of ground elevation. The lowest elevation of the entrance among all the tunnel nodes in the map of Fig. 8 was taken as the starting elevation for flooding, and five gradients of 1 m, 2 m, 3 m, 4 m and 5 m

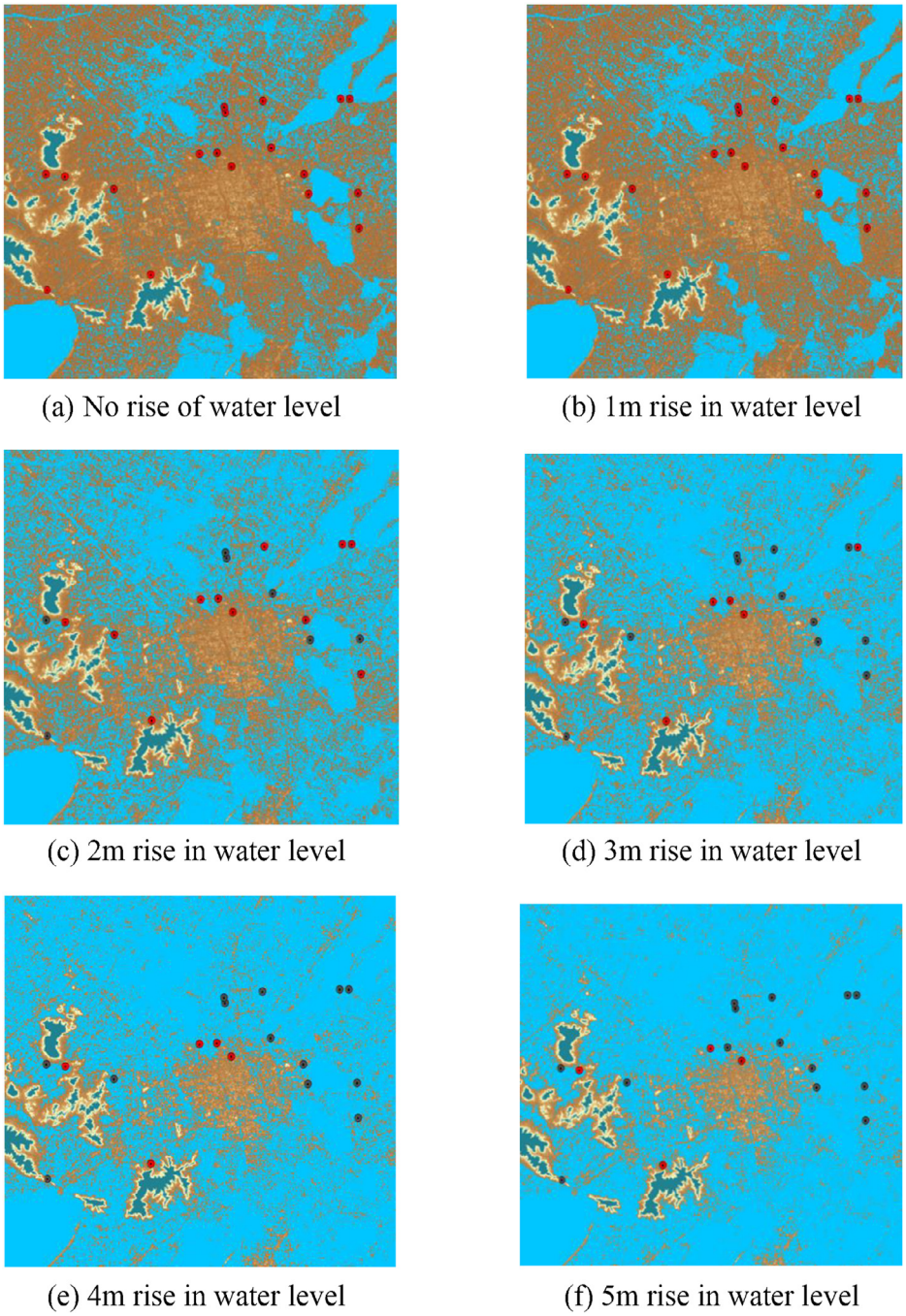

Fig. 9. Inundation map of road tunnels under different flood levels.

were set to obtain the inundation map under each gradient, as shown in the Fig. 9. Then the failure of any specific road tunnel in the road tunnel network under extreme heavy rainfall is evaluated by comparing the predicted flood water level caused by heavy rainfall with the elevation at the specific tunnel nodes.

Fig. 9 shows the inundation of tunnels under the continuous rise of different flood water levels. Red nodes represent undamaged tunnels, black nodes represent flooded tunnels, blue areas represent inundated areas caused by heavy rainfall, and the rest represent unflooded areas at different elevations. Fig. 10 shows the changes of inundation numbers of tunnels under different water level rises. It can be seen that before the water level reaching to 3 m, the number of tunnel failures increases rapidly. When the water level rise is over 3 m, two thirds of the road tunnels are flooded.

Based on the inundation of tunnels under heavy rainfall conditions, the damage on the topography and the associated decreasing of the road tunnel operational network efficiency are further analyzed. By removing damaged road tunnel nodes and related lines, Fig. 11 shows the damage of road tunnel topological network structure under heavy rainfall corresponding to the water level rise increasing from 1 m to 5 m, respectively. It can be found that the damage of network structure mainly occurs before the flood water level rises 3 m, which is the early stage of heavy rainfall disasters, and the damage of network structure is especially serious when the water level is 2–3 m. This is because most of the tunnel nodes are located at this elevation.

Fig. 12 shows the variation of road tunnel network efficiency and the network performance with the increasing of flood water level rise from 0 m to 5 m, e.g., Fig. 12a is referred to the network efficiency E_f by

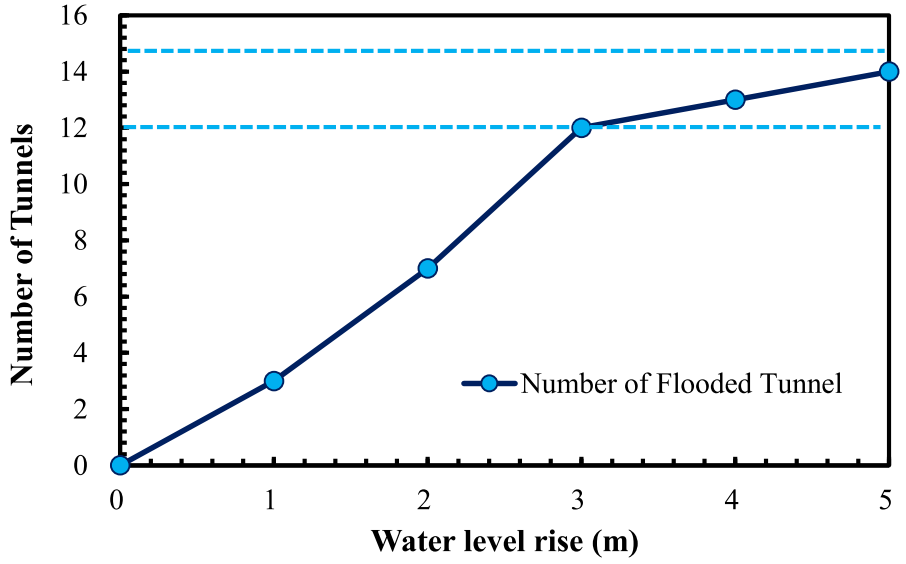

Fig. 10. Inundated number of tunnel nodes at different flood levels.

Eq. (7) and Fig. 12b is referred to the network performance Q by Eq. (8). It can be seen that both the decrease of the network efficiency E_f and the performance Q mainly occurs before the water level reaching to the level of 3 m, which is the evidence of the damage of the topographical structure in Fig. 11. In this stage, the global network efficiency decreases by nearly 20% represented by the decrease of 20% in performance Q, and it decreases by nearly 10% when the water level is 2–3 m. In the subsequent flood water level rise, the decrease of network efficiency is slightly gentle, about 3%. Heavy rainfall extreme weather can cause a lot of damage to the entire road tunnel network, and corresponding protective measures must be taken in the early stage of the disaster to avoid a sharp decline in the operation efficiency.

5.2. Resilience enhancement by adaptive design strategy

It is the ideal case that the water level rise could be precisely predicted by the above analysis and the resilience analysis could directly guide the evaluation and recovery from the impact by flood hazard. However, the true world always tells people that the future climate change is extremely uncertain or even is arguable these days. Thus, the uncertainty associated with the flood condition is not completely predictable and quantifiable. Bearing this design philosophy in mind, it is extremely important to propose and explore the value of the adaptive design methods such as the *observational method* (OM) and adaptive risk management as a central tenet of a new paradigm for engineering practice [36].

The smart sensing technique, e.g., wireless sensing network (WSN), nowadays is becoming an effective way to implement a real-time monitoring on the structural health state [37]. The idea whether the smart sensing in some way can assist in the decision for preventive maintenance is not explicitly explained so far, but engineers have a rough idea that it might do help to the enhancement of the timely monitoring. It is great that the time cost to recover the performance of UI, i.e., the rapidity, is a crucial dimension in assessing the resilience of underground infrastructure. The smart sensing could increase the response time of disruption of infrastructure and further increase the rapidity of recovery. If there is an ideal structure that its performance does not degrade with time t as shown in Fig. 13. In other words, the performance Q is always equal to unit. However, once the infrastructure is unfortunately disrupted by extreme hazard at time t_i, the performance has been reduced to f_d (f_d<1) through a period of time ΔT_1. After implementing the repair measures on the disrupted infrastructures, the performance has been recovered to normal state (i.e., $Q = 1$) through a period time of ΔT_2. By applying the resilience metric mentioned by Eq. 1, the calculated resilience index R_{e1} is expressed as below:

$$R_{e1} = \frac{1 + f_d}{2} \tag{9}$$

In this benchmark problem, if the smart sensing technique could be used before the disruption happens, the reduction of performance could be captured once it is being reduced. Thus, suppose the time period for infrastructure response time in this case of applying smart sensing equal to $1/n$ times ΔT_1, as shown in blue arrow line in Fig. 13. By applying the same repair measures, the recovery duration could also be $1/n$ times ΔT_2 on the basis of geometric laws. In other words, by applying the same repair measures, the rapidity of recovery by using smart sensing could be n times faster than the traditional monitoring system. It could be derived further that the area of performance loss in Fig. 13 for the smart sensing case could be n^2 times smaller than that for the traditional sensing case. The resilience index R_{e2} for the smart sensing case could be generally n^2 times larger than the R_{e1} for traditional sensing case and is represented as below:

$$R_{e2} = 1 - \frac{1}{2n^2}(1 - f_d) \tag{10}$$

Given the robustness performance f_d after the disruption at the level of 0.8, 0.5, 0.3 and 0.1, by applying Eq. (10), the calculated index R_{e2} for smart sensing case could be plotted against the relative response time coefficient n in Fig. 14. It is clear from the figure that the coefficient n could greatly affect the results of R_{e2}. If n is larger than 5, the resilience could be incredibly high and almost equal to unit. That is to say, the infrastructure performance could be strongly resilient, regardless of the vulnerability under disruption. This is the reason that the smart sensing could improve the infrastructure resilience even with the same repair or rehabilitation techniques. Table 3 has summarized the overall effects of smart sensing on resilience expressed by using relative response time coefficient n. Since the loss of resilience is related to second order of n, i.e., $\Omega(n^2)$, it thus could clearly indicate the great effect of smart sensing on the infrastructure resilience.

5.3. Other engineering measure to recovery from flood hazard

Besides the observational method discussed in the above, other adaptive design strategy under flood can be divided into engineering design strategy and non-engineering design strategy. The adaptive design strategy can follow the engineering treatment as below:

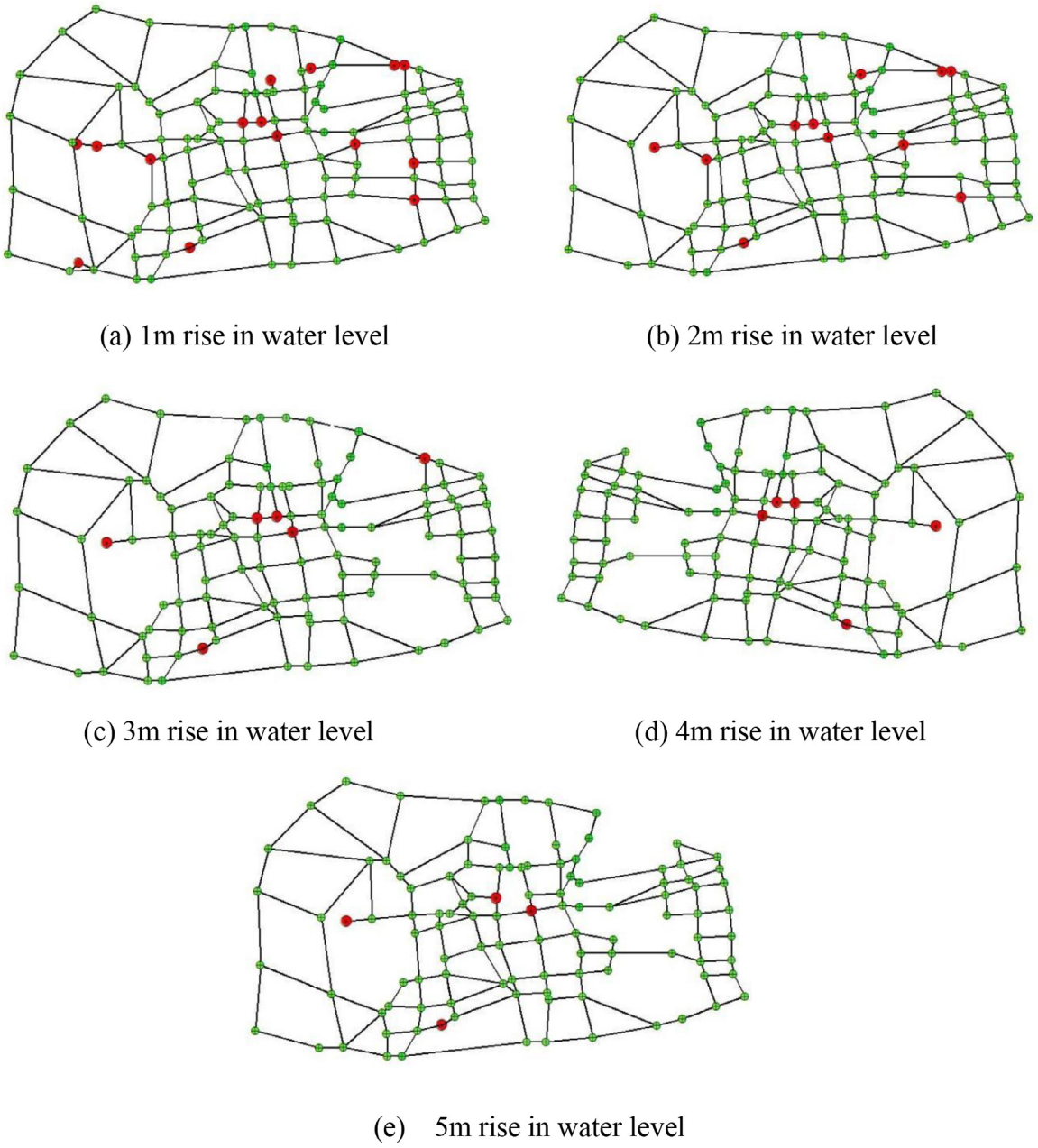

Fig. 11. Damage of road tunnel topological network at different flood levels.

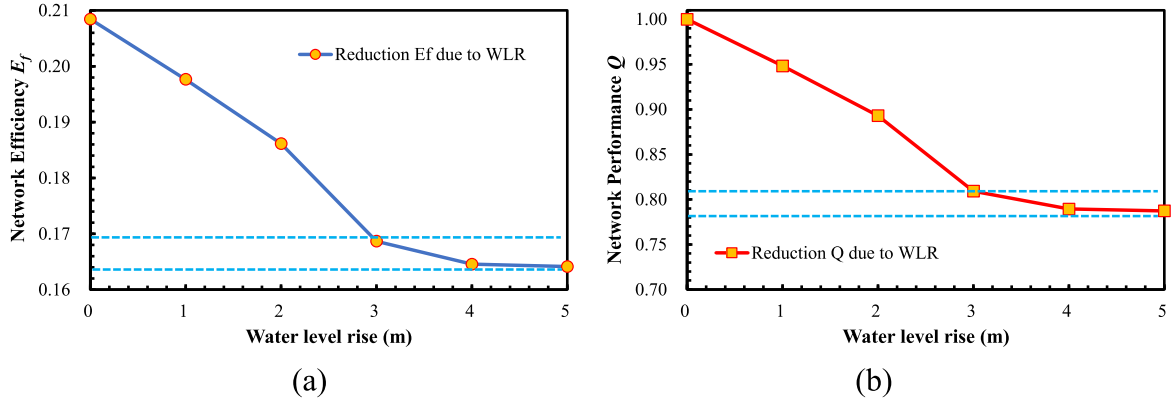

Fig. 12. Global network efficiency of road tunnel network.

Table 3
Comparison of resilience dimension between smart sensing and traditional sensing .

Dimension	Effect of smart sensoring
Response duration	$1/n$
Vulnerability	$1/n$
Robustness	$A - B/n$
Rapidity	$1/n$
Resilience	$C - D/n^2$
Resilience loss	$1/n^2$

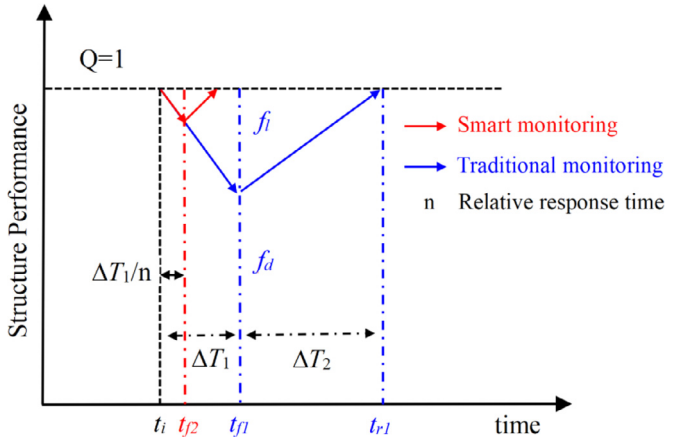

Fig. 13. Performance transition curves between smart sensing and traditional monitoring.

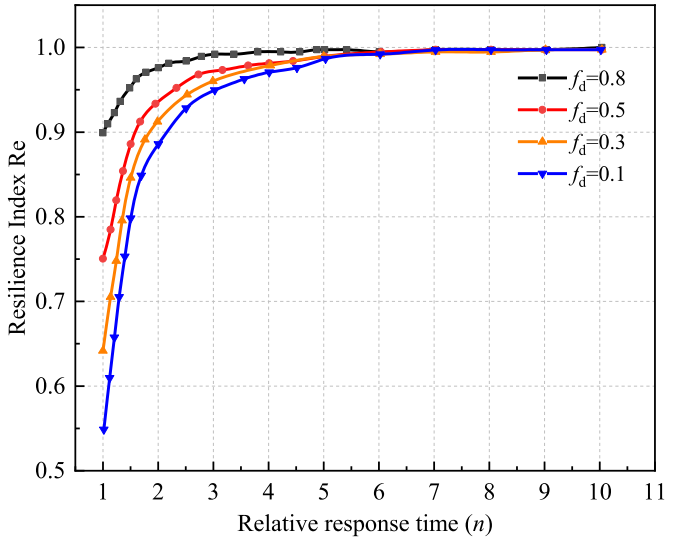

Fig. 14. Effect of rapidity of response time by using smart sensing on the tunnel resilience.

(a) The elevation of the entrance and exit of the underground infrastructure could be flexibly uplifted based on the dynamic precast of the local maximum flood level.
(b) The flood control and drainage standard of underground infrastructure in each section should be determined according to the maximum flood inundation that may be encountered in the area.
(c) Flood prevention measures shall be arranged at the entrance and exit to prevent flood backflow.
(d) The drainage ditches and steps should be designed outside the entrance of underground infrastructure or make the ground near the entrance have a certain slope.
(e) At the lowest part of the underground infrastructure, a drainage pump station is critically set to discharge the water in time.
(f) It is recommended to build a large-scale underground water storage system in the deep underground infrastructure to comprehensively solve the problem of flood in the wet season and water shortage in the dry season.

6. Conclusion

The underground infrastructure has a fast development over the past decades. The large scale of this typical civil infrastructure requires the resilience analysis modeling to consider both at the structural level and the system level. In particular with the age of climate change circles, multiple hazards either from the natural side or from the man-made side could give an impact on the basic performance of the underground infrastructure. In view of this condition, this paper has presented a general framework of the resilience analysis model to cope as much as possible with the above different factors. Several concluding remarks can be drawn as below:

(1) The resilience of underground infrastructure is defined to reflect the ability of the system to absorb the disruption caused by multi hazards and the corresponding ability to recover to an engineering practical level of the structural performance or system performance. The metric of resilience of UI can be visually explained by the ratio of the area for the performance function at the disruption stage $f(t)$, evolution stage $s(t)$ and recovery stage $r(t)$, over the area of normal performance function $Q_n(t)$.
(2) The performance indicators Q of the underground infrastructure subjected to the multiple hazards such as seismic, human-related engineering disturbances and flood are presented from the structural level in terms of fragility function, horizontal deformation and structural potential energy to system level in terms of the network efficiency double weighted by the physical length and the passenger volume of the underground infrastructure.
(3) Two typical examples of resilience analysis for underground infrastructures are illustrated from the structural seismic resilience to the network resilience. The seismic resilience evaluation for typical Shanghai metro tunnel under different seismic intensity *PGA* is discussed. It is found that the tunnel in Shanghai soft clay has a high resilience under the designed *PGA* level in practice.
(4) A typical city road tunnel network is selected as the application example to show the use of the framework of the proposed resilience model with emphasis on the network resilience. The vulnerability of the network performance in terms of the network efficiency is analyzed given different water level rises. Furthermore, the adaptive design strategy by using the real-time monitoring as the observational method is proposed to enhance the network resilience, which is mathematically proved to be effective.

However, although this paper has presented the performance of the underground infrastructure subjected to different types of the natural and human-related hazards. The coupling effect or the cascading effect of multi hazards is not considered at this moment, which is quite necessary to make the evaluation of the risk and resilience of the infrastructure more practical. It should be the next step of the authors' future works.

Declaration of Competing Interest

The authors declare that they have no known competing financial interests or personal relationships that could have appeared to influence the work reported in this paper.

Acknowledgment

This work is substantially supported by the National Natural Science Foundation of China (No. 52130805, 51978516, 52022070,

52108381), the National Key R&D Program (No. 2021YFF0502200 and 2021YFB2600804). The financial support is gratefully acknowledged.

References

[1] Chinese Academy of Engineering Strategic Consulting Center (CAE-SCC) Annual report on the development of china urban underground space in 2021. Beijing: Chinese Academy of Engineering; 2022.

[2] Moser CON. The asset vulnerability framework: reassessing urban poverty reduction strategies. World Dev 1998;26(1):1–19.

[3] Nyman MR, Johansson M. Merits of using a socio-technical system perspective and different industrial accident investigation methods on accidents following natural hazards – a case study on pluvial flooding of a Swedish railway tunnel 2013. Int J Disaster Risk Reduc 2015;13:189–99.

[4] Zhang MY, Pei WS, Lai YM, et al. Numerical study of the thermal characteristics of a shallow tunnel section with a two-phase closed thermosyphon group in a permafrost region under climate warming. Int J Heat Mass Transf 2017:952–63.

[5] ASCE MOP 144 Hazard-Resilient Infrastructure: analysis and Design 2021. https://ascelibrary.org/doi/book/10.1061/9780784415757.

[6] The Bridge 2019;49 (2) : 2019. https://www.nae.edu/File.aspx?id=212260.

[7] Shen YS, Gao B, Yang XM, et al. Seismic damage mechanism and dynamic deformation characteristic analysis of mountain tunnel after Wenchuan earthquake. Eng Geol 2014;180(8):85–98.

[8] Wang K, Wu Y, Fan QD. Construction of rainstorm security pattern based on waterlogging prevention and control: a case study on Zhengzhou City. Alex Eng J 2022;61(11):8911–18.

[9] Zhang WG, Han L, Gu X, et al. Tunneling and deep excavations in spatially variable soil and rock masses: a short review. Underground Space 2022;7(3):380–407.

[10] Shi JW, Liu GB, Huang P, et al. Interaction between a large-scale triangular excavation and adjacent structures in Shanghai soft clay. Tunnelling Underground Space Technol 2015;50:282–95.

[11] Krupa J, Jones C. Black Swan Theory: applications to energy market histories andTechnologies. Energy Strat Rev 2013;1(4):286–90.

[12] Lu XZ, Liao WJ, Fang DP, et al. Quantification of disaster resilience in civil engineering: a review. J Saf Sci Resilience 2020;1(1):19–30.

[13] Ayyub BM. Practical Resilience Metrics for Planning, Design, and Decision Making. ASCE-ASME J Risk Uncertainty Eng Syst 2015;1:3.

[14] Huang HW, Zhang DM. Resilience analysis of shield tunnel lining under extreme surcharge: characterization and field application. Tunnelling Underground Space Technol 2016;51:301–12.

[15] ASCE Committee on Critical Infrastructure Policy statement 518 - Unified definitions for critical infrastructure resilience. USA: ASCE; 2006.

[16] National Academy of Sciences of United States Disaster resilience: a national imperative. WashingtonDC: The National Academies Press; 2012. doi:1017226/13457.

[17] Tierney K, Bruneau M. Conceptualizing and measuring resilience: a key to disaster loss reduction. TR News 2007;250:14–17.

[18] Attoh-okine NO, Cooper AT, Mensah SA. Formulation of resilience index of urban infrastructure using belief functions. IEEE Syst J 2009;3(2):147–53.

[19] Capacci Luca, Biondini Fabio, Frangopol Dan M. Resilience of aging structures and infrastructure systems with emphasis on seismic resilience of bridges and road networks: Review. Resilient Cit Struct 2022;1(2):23–41.

[20] Singh Rohit Ranjan, Bruneau Michel, Stavridis Andreas, et al. Resilience deficit index for quantification of resilience. Resilient Cit Struct 2022;1(2):1–9.

[21] Sangaki AH, Rofooei FR, Vafai H. Probabilistic integrated framework and models compatible with the reliability methods for seismic resilience assessment of structures. Structures 2021;34:4086–99.

[22] Mottahedi A, Sereshki F, Ataei M, et al. Resilience estimation of critical infrastructure systems: application of expert judgment. Reliab Eng Syst Saf 2021;215:107849.

[23] Ayyub BM. Systems Resilience for Multi-hazard Environments: definition, Metrics, and Valuation for Decision Making. Risk Anal 2014;34(2):340–55.

[24] Yang TY, Lepine-Lacroix S, Ramos Guerrero JA, et al. Seismic performance evaluation of innovative balloon type CLT rocking shear walls. Resilient Cit Struct 2022;1(1):44–52.

[25] Castillo Juan Gustavo Salado, Bruneau Michel, Elhami-Khorasani Negar. Seismic resilience of building inventory towards resilient cities. Resilient Cit Struct 2022;1(1):1–12.

[26] Huang ZK, Pitilakis K, Tsinidis G, Argyroudis S, Zhang DM. Seismic vulnerability of circular tunnels in soft soil deposits: the case of Shanghai metropolitan system. Tunnelling Underground Space Technol 2020;98:103341.

[27] Huang ZK, Zhang DM, Pitilakis K, Tsinidis G, Huang HW, Zhang DM, Argyroudis S. Resilience assessment of tunnels: framework and application for tunnels in alluvial deposits exposed to seismic hazard. Soil Dyn Earthquake Eng 2022 (under review.

[28] von Ferber C, Holovatch T, Holovatch Y, et al. Public transport networks: empirical analysis and modeling. Eur Phys J B 2009;68:261–75.

[29] Latora V, Marchiori M. Efficient behavior of small-world networks. Phys Rev Lett 2001;87(19):198701.

[30] Zhang YJ, Ayyub BM, Saadat Y, Zhang DM, Huang HW. A double-weighted vulnerability assessment model for metro rail transit networks and its application in Shanghai metro. Int J Crit Infrastruct Prot 2020;29:100358.

[31] Huang ZK. Resilience Evaluation of Shallow Circular Tunnels Subjected to Earthquakes Using Fragility Functions. Appl Sci 2022;12:4728.

[32] FEMA Hazus 4.2 SP3: hazus earthquake model technical manual. FEMA; 2020.

[33] Chen YY, Li JM, Chen A. Does high risk mean high loss: evidence from flood disaster in southern China. Sci Total Environ 2021;785:147127.

[34] Shi J, Cui L, Tian Z. Spatial and temporal distribution and trend in flood and drought disasters in East China. Environ Res 2020;185:109406.

[35] Zhang D, Shi X, Xu H, et al. A GIS-based spatial multi-index model for flood risk assessment in the Yangtze River Basin, China. Environ Impact Assess Rev 2020;83:106397.

[36] Ayyub BM. Climate-Resilient infrastructure: adaptive design and risk management. Committee on Adaptation to a Changing Climate, ASCE; 2018. doi:101061/9780784415191.

[37] Huang HW, Xu R, Zhang W. Comparative Performance Test of an Inclinometer Wireless Smart Sensor Prototype for Subway Tunnel. Int J Archit, Eng Construct 2013;2(1):25–34.